# Optimization of Tetrapolar Impedance Electrodes in Microfluidic Devices for Point of Care Diagnostics using Finite Element Modeling

Martin Hantschke, Dimitrios Sideris, Panayiotis A. Kyriacou, and Iasonas F Triantis, *Member, IEEE*

***Abstract*— Electrophoresis is widely applied in the field of biochemistry and molecular biology. Tetrapolar electrical impedance sensing (TEIS) has been shown capable of replacing the conventional detection technology in order to develop a point of care electrophoretic analyzer. Besides the advantages of reduced influence of electrode polarization, TEIS is affected by sensitivity distribution depending on the electrode design. A well reported practice outside of electrophoresis, systematic investigation of the effects of sensitivity distribution on the TEIS in microfluidic devices has not been conducted. Here we utilize finite element modeling, backed by experimental results, to optimize the sensor design within an electrophoretic separation device. Numerous sensor designs were validated regarding detectability, sensitivity and spatial resolution. The results show, that minimizing the distance between the central/pick-up electrodes increases sensitivity and spatial resolution whereas the distance between the central electrodes and the outer electrode do not influence sensitivity and spatial resolution.**

## I. Introduction

Point of care (POC) diagnosis, the medical analysis carried out in-situ, close to the patient often at the time of consultation, is especially important in urgent care when timely decisions can improve clinical outcome, patient safety and satisfaction. Due to changing health care requirements, the demand for POC analysis is steadily growing [1]. POC has, in some sectors like blood glucose measurement or blood gas analyzers already improved the lives of millions of patients worldwide. Capillary electrophoresis (CE), the separation of dissolved molecules in a micro-channel using high voltage DC field is a powerful analytic process, capable of fast, highly efficient analysis of small sample volumes in complex samples [2]. CE and its variant Microfluidic chip electrophoresis (ME) are in particular advantageous for development into an automated, cost-effective and portable POC device.

However, fluorescence detection, the most widely used detection method, requires most biological samples to be labeled with a fluorescence marker [3]. This is a potential hazardous and cumbersome process not fit for use in clinical POC environment [4]. Electrical impedance and in some cases conductivity measurement, the measurement of electrical properties of the analytes, is advantageous because it allows for label-free detection of the analytes, which in turn allows for small detector assemblies compatible with portable devices and is cost effective. It has been reported for detection of biological species of electrophoretically separated samples. Studies [5], [6] have shown the possibility and significance of electrophoretic POC devices. Nevertheless, most of these sensors were of bipolar configuration, using the same electrodes to inject current and measure the voltage response [7]. Throughout literature outside of this particular field it has been well established, that tetrapolar impedance sensing (TEIS) is superior to its bipolar counterpart. TEIS involves four electrodes, two for current injection (called current carrying (CC) electrodes) and two for measurement of the voltage response (called pick-up (PU) electrodes). Using a tetrapolar setup allows the measured value to be related almost entirely with the analyte properties while eliminating the - often overwhelmingly higher - electrode impedance contribution to the measurement.

On the other hand, besides these advantages, TEIS also exhibits unique sources of error (e.g. negative sensitivity fields) that can only be overcome through systematically designing the electrode topology parameters that precisely suit a specific application. [8] Laugere at al [9] has presented an electrophoretic separation system using TEIS confirming its superiority by comparing with a bipolar system, however, the study does not involve analytical sensor design.

In this paper FEM modelling is used to validate, that specific parameters of electrode design can vastly improve the performance of an impedance-based ME system. Systematic investigation of the effects of electrode design in TEIS has been presented outside of electrophoresis that can be built on, however it does not involve considerations unique to electrophoresis i.e. micro channels and moving samples [10].

The authors are convinced that a practical POC ME device can only be achieved if a methodical approach to TEIS is adopted, thus optimizing sensitivity and detectability.

## II. Methodology

### A. Experimental section

A microfluidic separation device was produced in cooperation with Genetic Microdevices Ltd. A glass mold with the channel structure (85 µm x 15 µm x 60 mm) was produced using photolithography and wet etching. The mold was transferred via hot embossing onto PMMA (Polymethylmethacrylate) substrate of 3 mm thickness.

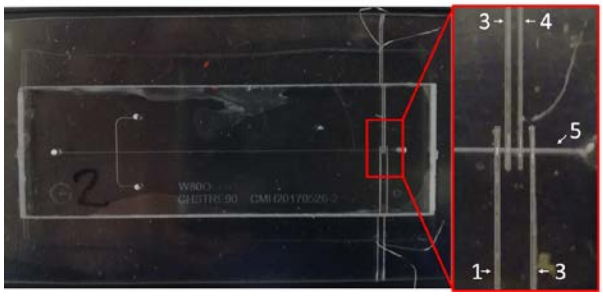


Figure 1 Microfluidic device (sensor area magnified) 1&2: CC electrodes, 3&4 PU electrodes, 5 microfluidic channel

M. Hantschke, Panayiotis A. Kyriacou and I. Triantis are with Department of Electrical and Electronic Engineering, City, University of London, Northampton Square, London EC1V 0HB, T: +44 (0)20 7040 3878, United Kingdom martin.hantschke.1@city.ac.uk, i.triantis@city.ac.uk

D. Sideris is with Genetic Microdevices Ltd., Unit 6, Princess Mews, Horace Road, Kingston upon Thames, Surrey, KT1 2SZ dimitrios.sideris@genetic-microdevices.co.uk

Prior to joining of the top substrate and bottom substrate, using heat and solvent bonding, four 80 µm platinum micro wires were pressed into the bottom substrate of the microfluidic device. The wires appear level with the surface of the bottom substrate and create a sensor area of 85 µm x 80 µm. The produced chip and a magnified sensor area can be seen in Fig. 1.

Sodium-Chloride (NaCl) solution, commonly called buffer, with a concentration of 154 mM was diluted with deionized water to create varying concentrations and manually injected via a syringe. Between measurements the microchannel was emptied and flushed with 5 ml deionized water. Measurements were taken with Precision LCR Meter E4980A (Keysight Technologies) using custom measurement leads connected directly to the ends of the micro wires.

### B. *FEM simulation*

Finite element models were created with COMSOL Multiphysics. In order to minimize computational resources only a 1mm x 1 mm excerpt, the sensor area (Fig. 1) of the microfluidic device, was simulated. Channel dimensions used in the model resemble to the fabricated device (15 µm x µm 85 x 1 mm). The material properties of PMMA as well as electrode material (platinum) have been added. Electrodes are created as rectangular shapes spanning the full width of the channel. This resembles the electrodes used in the experiments as well as a wide range of planar electrodes presented in literature. For reasons of simplicity and minimizing computational resources, electrodes in the presented simulations are created as boundary planes on the bottom side of the channel. NaCl buffer and its tenfold dilutions were simulated by fluid with corresponding conductivity values, acquired by measuring the conductivity of the prepared dilutions with Jenway conductivity Meter 3540.

### C. *Performance of sensor design parameters for varying concentrations*

Simulations were created with identical specifications to the ones mentioned before. Three different parameters were individually varied using parametric sweeps.(Fig. 2) Parameter ‘A’ the distance between PU electrodes (0 mm to 0.08 mm), parameter ‘B’ the distance between the CC electrodes and the PU electrodes (0 mm to 0.08 mm) and parameter ‘C’ the width of the electrodes (0 mm to 0.08 mm).

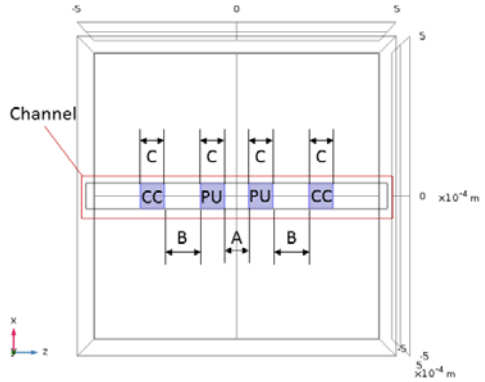


Figure 2. Image of the sensor area indicating the location of the channel and the CC and PU electrodes. Parameter A = distance between the PU electrodes, parameter B = Distance between PU and CC electrodes, parameter C = width of the electrodes

Each of these three series of parameter variations was performed for a channel filled with NaCL solution of varying concentration (154 mM to 15.4 mM).

### D. *Performance of sensor design parameters for localized concentration changers*

In order to simulate sample measurement a localized concentration change was introduced into the sensor area (Fig. 1). The sample is simulated as a box with the dimensions 85 µm x 85 µm x 15 µm filled with NaCL of increased concentration 155.54 mM, the remaining channel is filled with NaCl of 154 mM concentration. The width of the sample box is chosen identical to the injection channel width.

Injection via cross channel is the common procedure of sample introduction, which will produce an identical sized sample. At this point inhomogeneous concentrations within the sample due to diffusion and wall interaction are not taken into account. The elevated sample concentration of ca 1% is chosen according to simulations of concentrations distributions presented in a paper published by [11]. The sample box is placed in the center of the sensor area

### E. *Performance of sensor design parameters for simulated separation*

A sample box, identical to the one mentioned in the previous chapter, was placed in the channel and moved along the channel through center of the detector area via parametric sweep. The simulated impedance was recorded and plotted for 40 points (from z= -0.4 mm to z = 0.4 mm in 0.02 mm steps) within the channel. At this point, inhomogeneous concentrations within the sample due to diffusion and wall interaction are not taken into account.

The effect of the sensor design parameter A, varied in the same manner as described in the previous paragraph, on the spatial resolution of the sensor is intended to be investigated with this simulation of the moving sample. Parameter B = 0.02mm and parameter C = 0.08 mm. The meshing resolution of the channel has been increased from 1.8E-5 to 1.5E-6 in order to achieve more accurate results of localized concentration changes when moving the sample.

A second study was performed creating two identical samples with the distance of 0.15 mm between them to show that the CC electrode topology parameters affect the detectability of two samples moving in close proximity to each other.

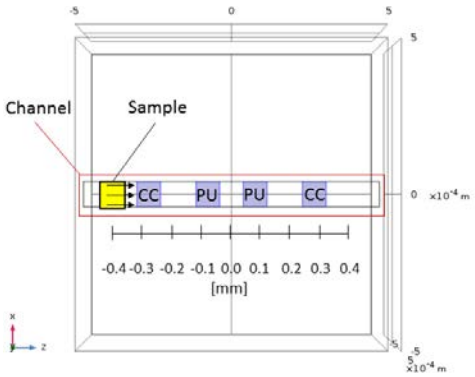


Figure 3. Image of the simulated sensor area with the sample (yellow) moving from z = - 0.4 mm to z = 0.4 mm

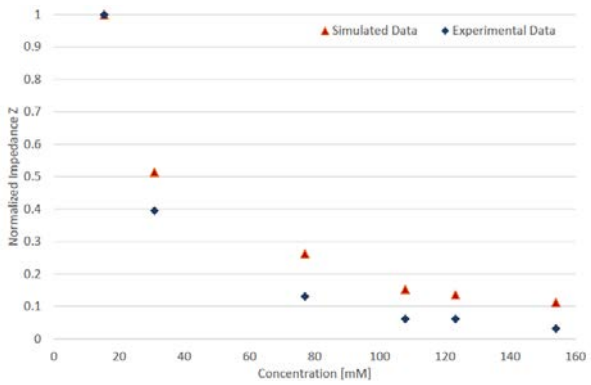


Figure 4. Impedance vs concentration, Experimental and Simulated data, normalized to maximum value

## III. Numeric Results and Discussion

### A. Results of experimental section

Fig. 4 shows the normalized impedance vs concentration graph of the experimentally acquired impedance values and identical simulations. The normalized impedance change for the measured and simulated impedance changes reflects the variations in concentration of the buffer solution. Both sets of impedance values show the same trend and give confidence in the viability of the numeric results.

### B. Performance results for varying concentration

Fig. 5 presents the simulated changes in impedance with changing buffer concentration for the variation of parameter A. The impedance values show the same exponential relationship as indicated by the measurements and simulations presented in Fig. 4. Increased concentration results in exponential lower impedance values as observed in studies using conductivity detection [12].

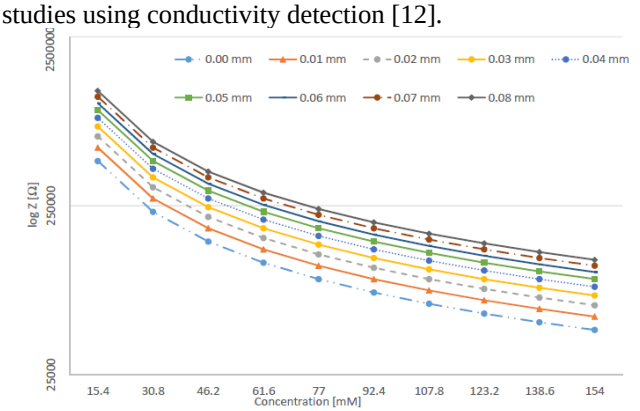


Figure 5. Impedance vs concentration for varying parameter A – distance between PU electrodes

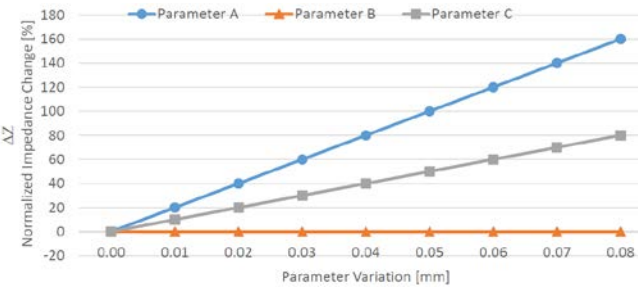


Figure 6. Impedance vs concentration for configurations varying parameter A – distance between the PU electrodes

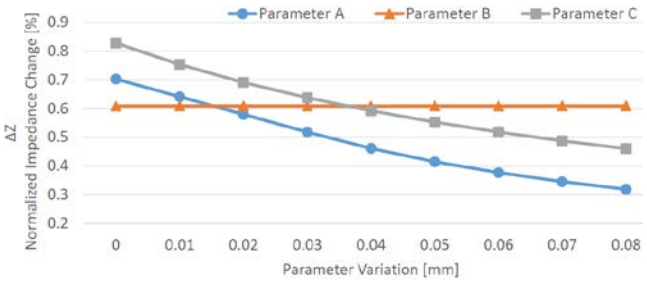


Figure 5. Impedance change vs design parameter change for a sample with 1% increased NaCl concentration

Furthermore, the variation of the design parameter has an influence on the simulated impedance presented in Fig. 6.

Identical simulations were conducted for sensor designs varying parameter 'B' – distance between PU and CC electrodes and variations of parameter 'C' – width of the electrodes. The results show the same trend as presented for parameter A as well as the same linear relationship between design parameter variation and impedance change. Increasing the distance 'A' between the PU electrodes from 0.02 mm to 0.18 increases the overall impedance simulated for this setup by 160%. The same behavior can be observed for variations of the electrode width 'C' where an width increase from 0.02 mm to 0.10 mm translates in an impedance increase of up to 80.1% for each variation. In contrary to this, an increase of distance 'B' between the CC and PU electrodes from 0.01 mm to 0.09 mm generates an impedance change of less than 1%.

The baseline impedance is depending on the concentration of the buffer solution as well as the location of the PU electrodes but does not seem to be significantly affected by the location of the CC electrodes. Therefore, they could be placed freely, for example at the openings of the channel, which would reduce the complexity of manufacture or the separation electrodes could be used as CC electrodes.

### C. Performance results for simulated sample

Fig. 7 shows the change of sensor response when placing the sample with a 1% increased NaCL concentration in the middle of the channel area, between the PU electrodes. The simulated impedance change caused by the sample ranges between 0.83% and 0.32% for the different sensor designs. In accordance with the results in the previous chapter, design variations 'A' and 'C' have influence on the sensitivity of the detector, where's 'B' (CC electrode distance) has no influence on the sensitivity. This shows that the design and the production tolerances for the PU electrodes have to be precise in order to ensure sensitivity of the system.

### D. Performance results for simulated separation

Fig. 8 presents the simulated sensor response of different designs for a sample (85 µm x 85 µm x 15 µm) that is moving through the sensor area from z = - 0.4 mm to z = 0.4 mm (Fig. 3). The full width at halve maximum (FWHM), a commonly used parameter to assess spatial resolution in signal processing, was calculated for each trace (Table I). To successfully distinguish between two samples the distance between those samples has to be bigger than the FWHM [13]. Spatial resolution is of greater relevance for ME where, due to generally shorter separation channel length, samples will arrive at the sensor less well separated. It is very important when separating samples with close electrophoretic mobilities.

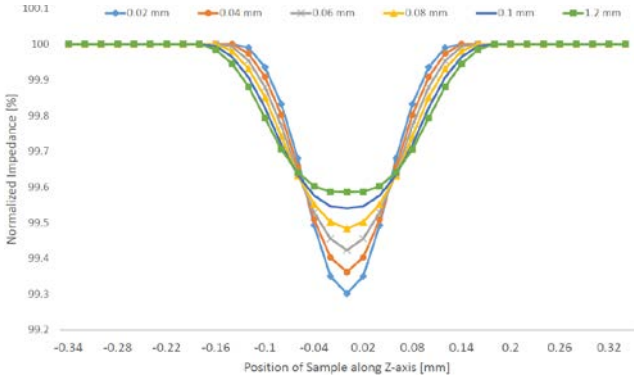


Figure 8. Simulated detector response of a simulated separation of a sample of 0.08 mm width. Plotted response for variations of design parameter A (CC electrode distance). Sensor response normalized.

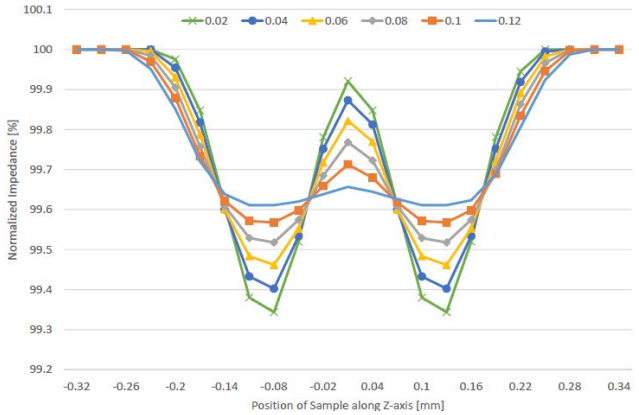


Figure *9*. Simulated detector response of separation of 2 bands of 0.08 mm width and 0.15 mm apart. Sensor response normalized.

It can be observed, that the shorter the distance between the PU electrodes the smaller the FWHM which means less well-separated samples are can be resolved leading to a better resolution of the system. The distance does not directly correspond to the size of the area between the PU electrodes but to the width of the high sensitivity area (Fig. 9), which in the case of the presented simulations, is slightly larger.

Fig. 10 presents the results of the simulated detector response of two samples traveling through the sensor area with a distance of 0.15 mm from each other. It can be observed, that for sensor designs with a smaller inter CC electrode distance and hence smaller FWHM the sensor response is much more detailed.

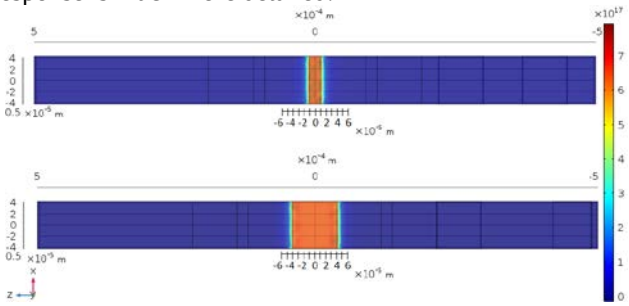

Figure 10 Sensitivity distribution for area between PU electrodes for different parameter A (distance between PU electrodes) Top A= 0.02 mm; Bottom A= 0.08 mm

TABLE I. SPATIAL RESOLUTION FOR DIFFERENT SENSOR DESIGNS

| **Spatial resolution for different sensor designs** | |
|---|---|
| ***Parameter C [mm]*** | ***FWHM [mm]*** |
| 0.02 | 0.114 |
| 0.04 | 0.127 |
| 0.06 | 0.142 |
| 0.08 | 0.16 |
| 0.10 | 0.18 |
| 0.12 | 0.199 |

## IV. CONCLUSION

The integration of tetrapolar electrical impedance sensing (TEIS) in electrophoretic separations presents a promising method to create a powerful analytical device that can still be portable. With the use of finite element modelling (FEM) we were able to systematically investigate electrode topology without the need of expensive and laborious manufacturing of the presented 22 sensor designs. The paper shows how specifically important the size and topology of the pick electrodes is for the detectability and resolution of TEIS in microchip electrophoresis. This knowledge will be fundamental for further investigations and improvement of the presented technology. Only with the systematic approach to sensor design shown in this work a detection system can be produced that can rival and potentially replace conventionally used fluorescence detection.

## REFERENCES

[1] A. St John and C. P. Price, “Existing and Emerging Technologies for Point-of-Care Testing.,” *Clin. Biochem. Rev.*, 35(3), pp. 155–67, 2014.
[2] W. R. Vandaveer IV, S. A. Pasas-Farmer, D. J. Fischer, C. N. Frankenfeld, and S. M. Lunte, “Recent developments in electrochemical detection for microchip capillary electrophoresis,” *Electrophoresis*, 25(21–22), 3528–3549, 2004.
[3] E. R. Castro & A. Manz, “Present state of microchip electrophoresis: state of the art and routine applications.,” *J. Chrom. A*, 1382, 66–85, 2015.
[4] K. A. Mahabadi, I. Rodriguez, C. Y. Lim, D. K. Maurya, P. C. Hauser, and N. F. De Rooij, “Capacitively coupled contactless conductivity detection with dual top-bottom cell configuration for microchip electrophoresis,” *Electrophoresis*, 31(6), 1063–1070, 2010.
[5] S. Staal *et al.*, “A versatile electrophoresis-based self-test platform,” *Electrophoresis*, 36(5), 712–721, 2015.
[6] A. P. Lewis *et al.*, “Review on the development of truly portable and in-situ capillary electrophoresis systems,” *Meas. Sci. Technol.*, 24(4), 2013.
[7] V. Šolínová and V. Kašička, “Recent applications of conductivity detection in capillary and chip electrophoresis,” *J. Sep. Sci.*, 29(12), 1743–1762, 2006.
[8] S. Grimnes and Ø. G. Martinsen, “Sources of error in tetrapolar impedance measurements on biomaterials and other ionic conductors,” *J. Phys. D. Appl. Phys.*, 40(1), 9–14, 2007.
[9] F. Laugere *et al.*, “On-Chip Contactless Four-Electrode Conductivity Detection for Capillary Electrophoresis Devices On-Chip Contactless Four-Electrode Conductivity Detection for Capillary Electrophoresis Devices”, 75(2), 306–312, 2003.
[10] P. Kassanos, A. Demosthenous, and R. H. Bayford, “Towards an optimized design for tetrapolar affinity-based impedimetric immunosensors for lab-on-a-chip applications,” *IEEE-BIOCAS*, 141–144, 2008.
[11] J. G. Alves Brito-Neto, J. A. Fracassi Da Silva, L. Blanes, & C. L. Do Lago, “Understanding capacitively coupled contactless conductivity detection in capillary and microchip electrophoresis” *Electroanalysis*, 17(13), 1207–1214, 2005.
[12] F. Hissner, J. Mattusch, & K. Heinig, “Quantitative determination of sulfur-containing anions in complex matrices with capillary electrophoresis and conductivity detection,” *J. Chrom. A*, 848(1–2), 503–513, 1999.
[13] G. W. Slater, C. Desruisseaux, & S. J. Hubert, “DNA Separation Mechanisms During Electrophoresis,” in *Capillary Electrophoresis of Nucleic Acids: Vol I:* Humana Press, 2001, 27–41.